

## **Modeling the Redistribution of Snow in Alpine Areas Using Geographic Information Processing Techniques**

D.W. CLINE

Department of Geography  
University of Colorado  
Boulder, Colorado 80309, U.S.A.

### **ABSTRACT**

The spatial distribution of snow in alpine landscapes is typically heterogeneous. This spatial variability may be caused primarily by surface features in the alpine which significantly affect the velocity of wind near the surface, and thus affect the capability of the wind to entrain, transport, and deposit snow. Such features include gross topography, affecting convergence and divergence of the wind flow over many tens of meters, and local topographic discontinuities which may cause acceleration or reduction of the wind velocity and possibly flow separation. In this study, the utility of spatial modeling techniques for providing information about the spatial redistribution of snow by wind for this alpine area is examined. Surface characteristics affecting snow distribution are identified and mapped for the Niwot Ridge area in the Colorado Front Range, using Remote Sensing and Geographic Information Processing techniques. These surface features are incorporated into a series of logistic regression models predicting the spatial extents of snowcover for each of seven unidirectional prevailing wind directions. Distinct patterns predicted by each model can be associated with a map of snowcover derived from a Landsat TM image.

### **INTRODUCTION**

The spatial distribution of snow in the alpine is typically heterogeneous. Perhaps the most visible manifestation of this is in alpine vegetation, where patterns develop according to the amount of soil moisture, length of growing season, nutrient fluxes, and exposure to wind and cold temperatures, all related to the distribution of snow. Less visible are soil moisture gradients, surface and subsurface water flow routing, and ensuing stream hydrochemical loadings which originate from areas of snow accumulation

(Swanson, *et al.*, 1988). Increased soil erosion rates associated with late-lying snow patches work to create new landforms (nivation hollows) in the alpine landscape (Thorn, 1974). Clearly, snow distribution is an important factor in both the development of alpine landscapes and the processes which occur there.

Little is known about natural variability of snow cover in this environment. In this landscape with a large degree of natural heterogeneity, it is uncertain whether a significant change in the snow redistribution process and the resultant patterns could be recognized. In this study, a series of "first approximation" models for the spatial distribution of snow in the alpine are developed to determine if simple mechanistic principles related to snow transport and deposition can be effectively modeled in a spatial context. The intent is not to provide an exhaustive treatment of complex snow transport mechanisms, or to attempt to include every conceivable variable within the model. Rather, its aim is to explore the utility of spatial modeling methods as a tool for understanding alpine snow distribution, and to provide an introductory assessment of the relative importance and sensitivity of a few general variables. A discussion of the model development is presented, including data acquisition and derivation, model formation, and an assessment of modeling results. Additionally, analysis of the sensitivity of the model to variations in wind direction is presented. Finally, a brief discussion on future directions for this modeling effort is provided. All techniques used in this project utilize operations commonly available in raster-based geographic information systems (GIS).

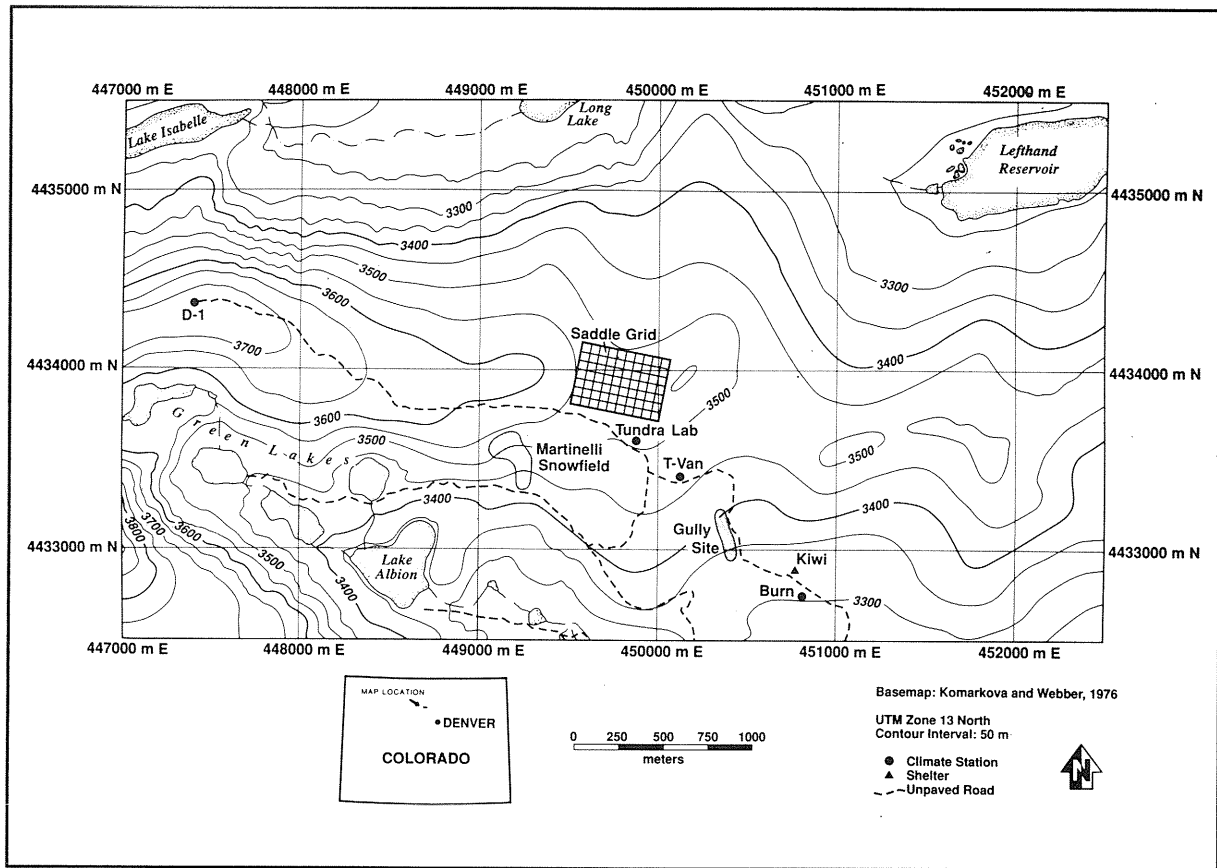


Figure 1. Map of Niwot Ridge study area, located in the Colorado Front Range of the Southern Rocky Mountains.

## METHODOLOGY

### Study Area

The area chosen for this study is Niwot Ridge, located in the Colorado Front Range of north central Colorado. It is an interfluvium extending approximately ten kilometers eastward from the Continental Divide, and is mostly above treeline. The study area itself is a 5.5 km x 3.0 km rectangle centered on the Saddle area of the Ridge (Figure 1). Many of the effects of the redistribution of snow in this alpine area have been documented by extensive geocological research performed here during the past several decades. Current research interests here include the effects of changing snowcover characteristics on alpine geocological systems.

Snowfall can occur on Niwot Ridge during any month of the year; seasonal accumulation typically begins sometime around early October.

Characteristically high winds provide a mechanism for rapid snow redistribution. Mean winter daily maximum winds typically range from  $20 \text{ m sec}^{-1}$  to  $25 \text{ m sec}^{-1}$ , with peak gusts frequently exceeding  $50 \text{ m sec}^{-1}$ . The maximum wind ever recorded on Niwot Ridge is  $92 \text{ m sec}^{-1}$  at the D1 Site. Significant snowfall occurs during the winter months, however the high winds make accurate snowfall measurement extraordinarily difficult. The resulting snow cover tends to be extremely heterogeneous, with protected areas receiving most of the deposition, while most exposed areas are scoured free of snow.

### Data Acquisition and Development

Snow transport and deposition is primarily a function of wind velocity and shear stress near

the surface (Radok, 1968; Kobayashi, 1972; Tabler, 1973; Berg and Caine, 1974; Takeuchi, 1980; Schmidt, 1982; Schmidt, 1986). Differential shear stress caused by non-uniformities in the flow create areas of erosion and redeposition of the snowcover, giving rise to the heterogeneous nature of the alpine snowpack. Given adequate velocity profiles, the surface shear stress may be calculated for specific points. However, an enormous array of instrumentation would be required to determine the spatial distribution of surface shear stress by use of velocity profile measurements for even a small alpine area (Olyphant and Isard, 1987), rendering this approach impractical. Alternately, surface characteristics affecting surface wind velocity and shear stress may be mapped, providing an estimate of the relative spatial distribution of surface wind velocities and shear stress, although this method cannot provide calculated values of shear stress such as those obtained through velocity profile analysis.

For the exploratory nature of this project, two surface characteristics affecting relative wind velocity were identified for mapping. The first is gross topography, affecting convergence and divergence of the wind flow over many tens of meters. The second characteristic is local topographic discontinuities, or small scale terrain features which may produce acceleration or reduced wind velocities and flow separation in localized areas. To provide information about sensitivity to wind direction, these two variables were needed for several prevailing wind directions. As multi-directional air flow, such as that caused by topographic steering of the wind was considered to be beyond the scope of this study, wind flow direction is assumed to be unidirectional for all cells of the model at one time. However, this single direction can be modified to examine the effects of different "prevailing" wind directions on the distribution of snow.

Using a digital elevation model (DEM), a digital terrain model (DTM) can be developed to provide information about gross topographic characteristics and small scale terrain features. From the elevations of individual cells of the DEM, a DTM of slope in relation to the prevailing wind can be generated. This slope model represents gross topography. Using this DTM, the second derivative of elevation, or change in slope between a particular cell and the cell adjacent to it can be calculated to determine

the magnitude of flow divergence and convergence for each cell, representing local topographic discontinuities. A subset of the U.S.G.S. Ward, Colorado DEM provided the necessary areal coverage for the project. The spatial resolution of this DEM was 30 m x 30 m. To prepare the elevation data for the wind direction analysis, the DEM was rotated by 15° increments into seven prevailing wind directions ranging from 225° SE to 315° NE using a bilinear interpolation rotation transformation. This range represents typical prevailing winds occurring during the winter season at Niwot Ridge, as shown in Figure 2.

### *Gross Topography*

Gross topography is defined here as the slope of a cell relative to a particular wind direction. The magnitude and sign of the slope can be calculated from a DEM. In this case, the sign reflects whether the slope is converging or diverging with respect to the wind. Slope is frequently derived from digital elevation data by examining the elevations of four or eight neighbors of a particular target cell (Skidmore, 1989). The use of several neighbors effectively smooths the terrain during the calculation of slope. This presents a problem since the second derivative of elevation, or rate of change of slope must subsequently be calculated for this study. Any smoothing applied to the DEM, either intentionally or inherent to processing techniques, necessarily reduces the magnitude of the rate of change of slope. To avoid this problem, the simplest calculation of slope was utilized here, involving only a particular target cell and one of its neighbors.

To calculate slope from the DEM, the elevation of a particular target cell and the elevation of a cell immediately "upwind" of it must be determined. A convolution (*i.e.* "moving window") filter is used to determine the elevation of each upwind cell and to place it in the same cell vector as the target cell. A 3 x 1 filter kernel with elements

$$|1|0|0|$$

is convolved with the DEM, and the sum of the filter elements is returned in a new matrix. When the convolution of the DEM is complete, the new matrix contains all DEM cell values shifted one cell to the right; the upwind cells are

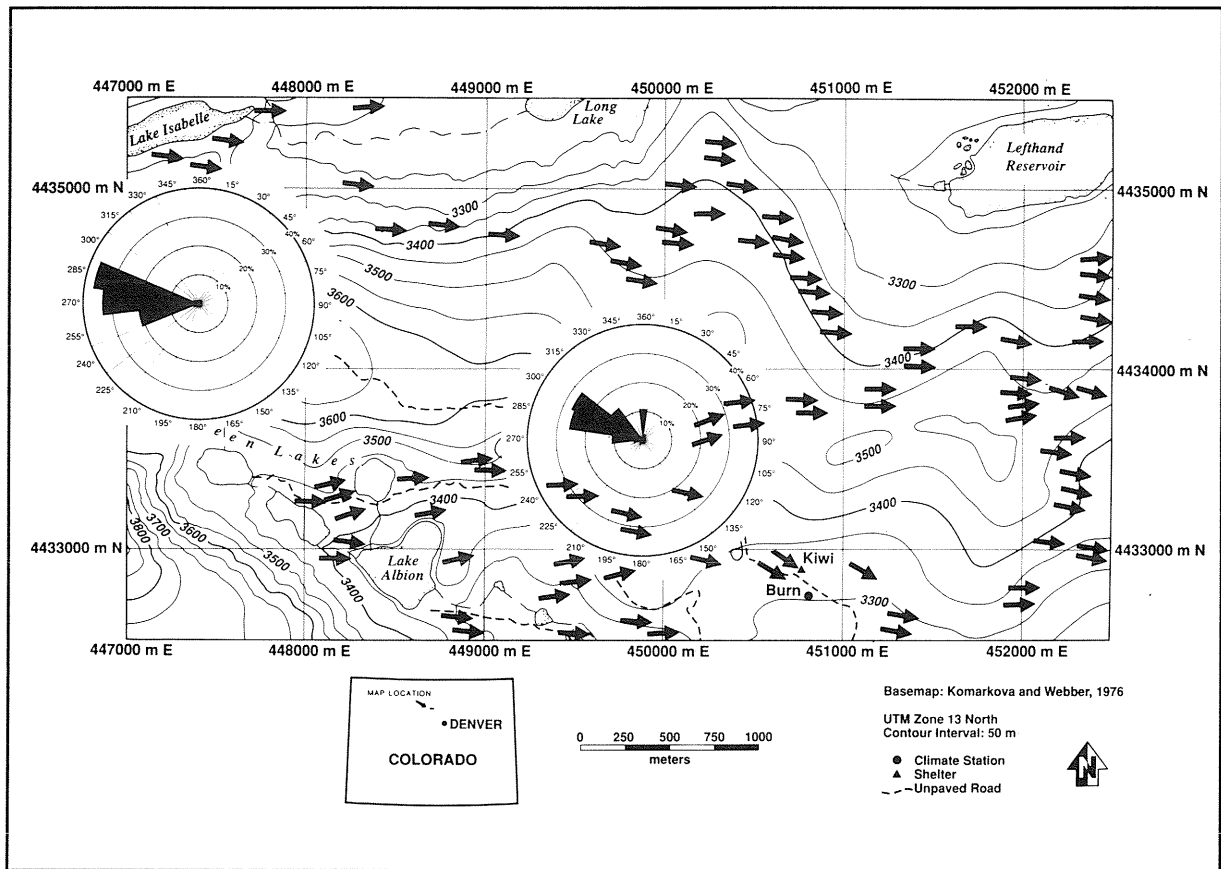


**Figure 2.** Prevailing winds are shown for the Saddle area. The wind roses were derived from data collected at the D1 Site and the Tundra Lab during the months of October and November, 1988 and 1989. The arrows represent the direction of krummholz flagging at treeline, reflecting long term winter prevailing winds (from Holtmeir, date unknown).

in the same cell vector as the target cell. By placing adjacent cells in the same cell vector as the target cells, mathematical operations between neighbors can be performed, in a manner similar to that proposed by Berry (1987). Other methods exist for examining the neighborhood of a target cell, but these methods typically search in a radial fashion outward from the target cell. The method developed for this study examines only the neighborhood immediately upwind or downwind of a target cell, *i.e.* in the same wind vector.

Once the elevation values of the upwind cell are placed in the same cell vector as the target cell the slope between the two can be determined. The slope is calculated using the equation

$$\text{Slope}_{\text{target}} = (\arctan((\text{Elevation}_{\text{target}} - \text{Elevation}_{\text{upwind}})/\text{cellsize})) * 57.2958 \quad (1)$$

The main structure of this expression is the difference in elevation between two cells (rise) divided by the cell size (run). The constant 57.2958 converts the result from radians to degrees. Values of 0 represent flat areas, negative values represent the magnitude of divergent slopes, and positive values represent the magnitude of convergent slopes.

It is important to note that this method of determining slope provides a value of slope that corresponds to the boundary of two cells, rather than the center point of any particular cell. The elevation values in the DEM reflect the value at the center of each cell. Since two center points

are used to derive slope, the resultant slope corresponds to the unit distance between the two center points.

#### *Local Topographic Discontinuities*

To derive the change in slope, a simple differencing operation must be performed using the slope of a target cell and the slope of a cell adjacent to it. Once again, this operation is initiated by placing the values of adjacent cells in the same cell vector as the target cells using the convolution filtering method described above, except the slope matrix is used in the convolution rather than the DEM. This time, however, the slope value of the *downwind* adjacent cell is used. By doing so, the resultant value of the change in slope corresponds once again to the center of the target cell. It is imperative that this operation be done in this manner to avoid misaligning the cell vectors.

Following the placement of adjacent downwind cells in target cell vectors, then the change in slope is calculated using the equation

$$\text{Slope Change}_{\text{target}} = \text{Slope}_{\text{downwind}} - \text{Slope}_{\text{target}} \quad (2)$$

Here, values of 0 correspond to no change in slope; negative values represent the magnitude of local slope divergence, and positive values represent the magnitude of local slope convergence.

#### *Development of Snowcover Map*

The modeling approach used in this project required a map of snow cover, from which samples could be extracted for model development, and which the resultant models could be compared against for assessment of performance. For this purpose, a Landsat Thematic Mapper image was obtained and processed to generate a map of snow cover for the study area. A scene acquired November 7, 1982 was considered suitable, since climatic conditions prior to this date were conducive to snow redistribution. Climatological data for the period prior and following the image acquisition are provided in Figure 3. During a 14 day period prior to the acquisition date of the TM image (Day 297 through Day 310), 56 mm of measured precipitation occurred. No measured precipitation occurred during the two days

immediately preceding the image acquisition, providing time for the last preceding snowfall to become redistributed. Wind velocities averaged over 12 m sec<sup>-1</sup> during this same 14 day period; the daily averages for the two days prior to the image date were 15 m sec<sup>-1</sup> and 17 m sec<sup>-1</sup>, with gusts exceeding 30 m sec<sup>-1</sup>. Temperatures during this two-week period ranged from a low of -21° C at the D1 Site to a high of 5° C at the Saddle Site. During the three-day period between the acquisition of the image and the previous snowfall, temperatures never exceeded freezing. Although solar insolation was much more variable at the higher D1 Site than at the Saddle Site prior to November 7, overall insolation at both sites was characteristically low due to the time of year. Essentially, the image acquisition was preceded by a period of snowfall followed by relatively high winds, subfreezing temperatures, and low solar insolation.

Preprocessing of the image included corrections for atmospheric effects and georeferencing the image to the UTM coordinate system. Training areas for classification were identified for four cover types: No Snow, Snow, Forest, and Ice-Covered Lakes. Using the visible and near-infrared bands, the image was then classified using a maximum likelihood classification technique. While most of the study area lies above treeline, some forested area exists in the margins of the study area. Snow cover within these forested extents could not be determined using satellite imagery, therefore they were excluded from further analysis. Similarly, the lakes within the study area were excluded.

The classified snowcover map is shown in Plate 1. No means of quantitatively assessing the accuracy of the classification exist, however subjective visual assessment indicated that the classification was generally very good. A qualitative accuracy assessment was deemed sufficient for the exploratory nature of this project.

#### **Model Development**

Given the categorical nature of the dependent variable (presence or absence of snow), a logistic multiple regression (logit) model was utilized. The independent variables used were the gross topography and local discontinuity datasets. A sample dataset was extracted from each of these two datasets, as well as from the snowcover dataset to develop the

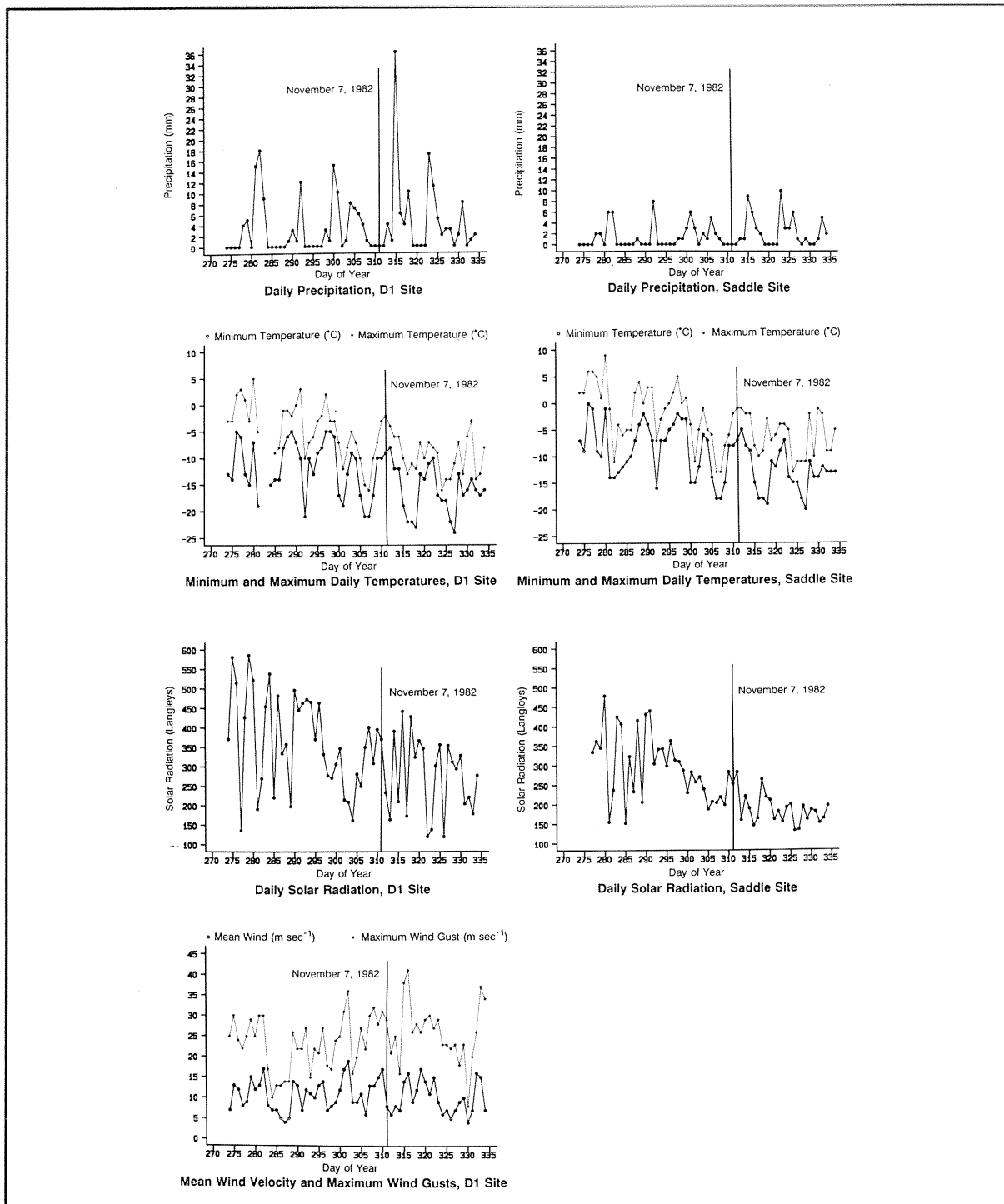


**Figure 3.** Climatic data are shown for October and November, 1982 (Losleben, 1983). November 7, 1982 is the date of image acquisition. Precipitation was measured with a weighing rain gauge protected by an Aiter shield and snow fence. Temperature was measured with a hygrothermograph. Solar insolation was recorded on a bimetallic strip actinometer. Wind velocity was measured with a three-cup anemometer.

logit model. The model was then applied to the remaining cells of the terrain datasets to determine a probability of occurrence of snow for each cell in the study area. Each cell was then classified as either Snow or No Snow by thresholding the probabilities to achieve maximum classification accuracy for each category. A logit model of this nature was developed for each of the seven prevailing wind directions.

#### *Data Sampling*

A systematic sampling strategy was utilized to obtain a representative sample of the dependent and independent variables. To insure that any spatial autocorrelation found in the error term would not be an artifact of the sampling, each of the independent variables were tested for spatial autocorrelation using the Moran's I statistic (Odlund, 1988). The Moran's I coefficient ranges from zero to one, with zero indicating no spatial autocorrelation and one indicating maximum spatial autocorrelation. As might be expected, gross topography demonstrated significant spatial autocorrelation for the first several lags. By the tenth lag, the Moran's I coefficient was reduced to 0.19, indicating that at distances of 300 m (10 cells) no significant spatial autocorrelation existed within the gross topography dataset. The local topographic variance exhibited much less spatial autocorrelation. Moran's I coefficients of close to zero were calculated by the third lag, indicating that spatial autocorrelation was insignificant at distances of 90 m (3 cells). The results of the Moran's I test indicated that a systematic sample drawn from the global datasets using a sampling interval of 10 cells would avoid significant spatial autocorrelation. Such a sample was then drawn from each of the seven global datasets for both gross topography and for local topography, as well as for the map of snowcover. This resulted in a total of 15 sample datasets of 180 cells each. Forty-four samples which occurred in areas of forest or lakes were discarded, leaving each sample dataset with 136 samples.

#### *Model Formation*

Using the sample datasets, seven logit models were developed, representing each of the seven prevailing wind directions. The categorical dependent variable used in each model was the presence or absence of snow. The independent

variables used in each model were the gross topography and the local topography corresponding to a given wind direction. The resulting logit models were then applied to the full datasets for each prevailing wind direction to produce maps of the probability of the presence of snow for each cell in the study area which was not forest or lake.

The probability of the presence of snow in any particular cell may range from zero to 100, however cells with low probabilities should be classified as no snow. An optimal probability threshold was desired which would result in the maximum number of correctly classified cells for both categories. The probabilities associated with cells of each category of the snowcover map may be used to determine a classification threshold (Pereira and Itami, 1991). The probability maps for each wind direction were compared to the map of snow cover using a cell by cell cross tabulation technique. Optimal probability thresholds for each wind direction were identified by examination of plots of the percentage of correctly classified cells in each category resulting from unit increases in probability (Figure 4).

## **RESULTS AND DISCUSSION**

The classification accuracies achieved by optimizing the probability thresholds are shown in Table 1. Although considered to be low, these results are encouraging. The use of only two simple explanatory variables to achieve these levels of accuracy suggests that refinements to this modeling approach may provide a method for improving understanding of alpine snow distribution.

The optimization method described above provides the most accurate classification on a cell by cell basis. Such cell by cell comparisons may not provide the best indication of the performance of predictive spatial models such as these, however, as such methods ignore qualitative differences between spatial patterns evident in the model (Turner, *et al.*, 1989). To better understand the effects that terrain may have on alpine snow distribution, a qualitative assessment of the model's performance is warranted. Such an assessment can be made by visual analysis of the snow distribution patterns predicted by each model. As well, visual analysis of maps of error resulting from each model is useful.

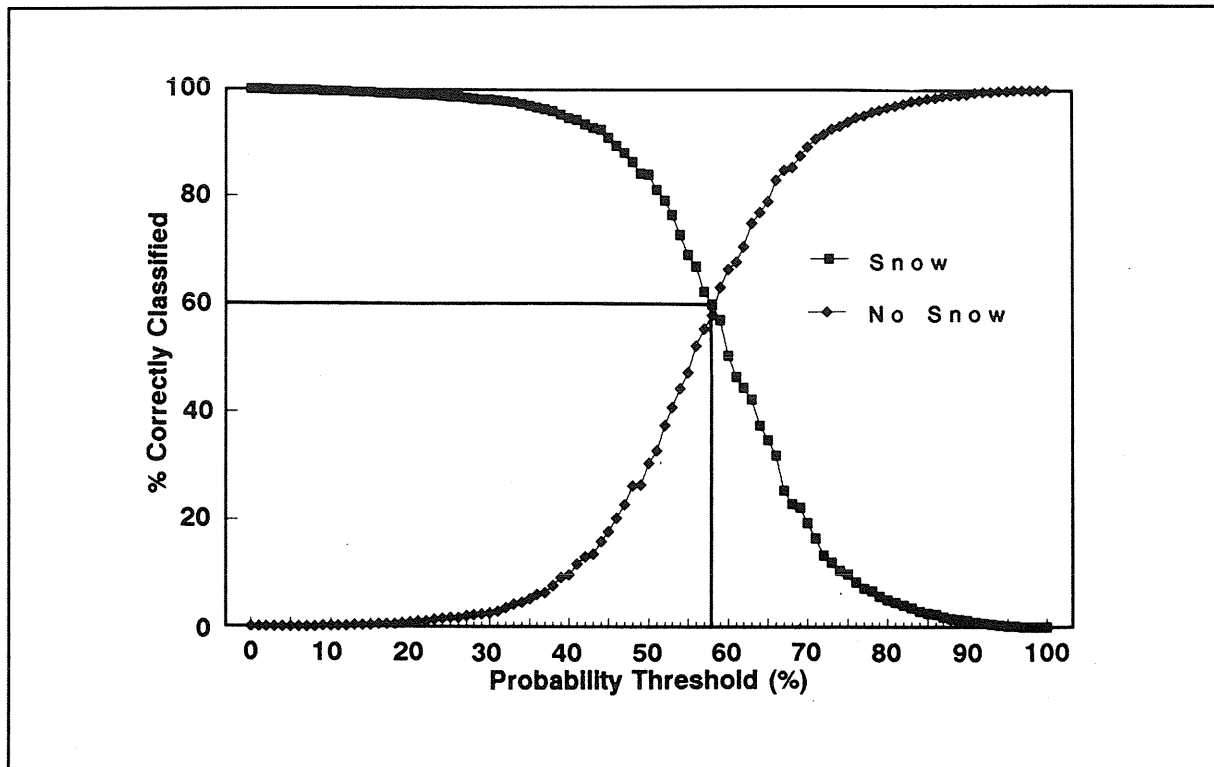
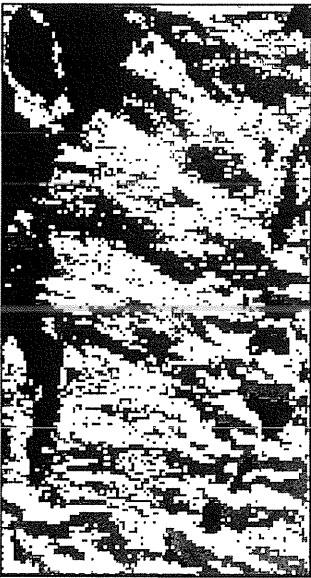


**Figure 4.** Optimal probability threshold for one of the wind direction models. If the probability map produced by the model is classified using the threshold  $p = .58$  ( $p < .58 = \text{no snow}$ ,  $p > .58 = \text{snow}$ ), 60% of the both the snow covered area and of the no snow area on the snowcover map will be correctly classified. Shifting the threshold to either the left or the right results in improved classification of one category at the expense of the other.

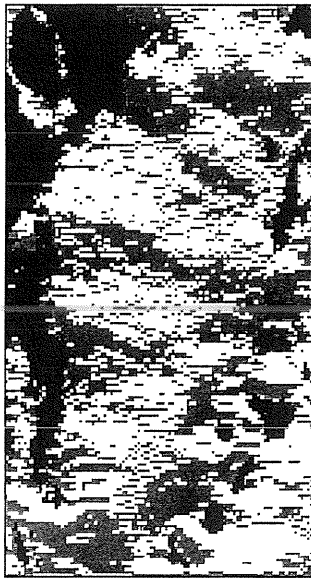
WIND DIRECTION	PROBABILITY THRESHOLD	CLASSIFICATION ACCURACY, NO SNOW	CLASSIFICATION ACCURACY, SNOW
225°	56 %	58.00 %	60.64 %
240°	57 %	58.33 %	63.13 %
255°	58 %	60.57 %	58.70 %
270°	58 %	57.97 %	60.02 %
285°	59 %	59.25 %	62.58 %
300°	58 %	58.29 %	58.24 %
315°	58 %	59.30 %	60.24 %

**Table One.** Classification accuracies for No Snow and Snow obtained by setting the threshold probability at the value shown.





WIND DIRECTION: 285°



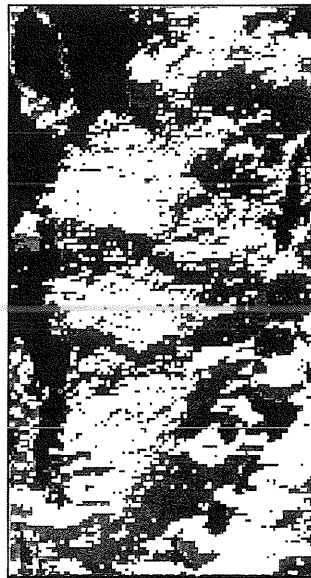
WIND DIRECTION: 270°



WIND DIRECTION: 300°



SNOWCOVER MAP, DERIVED FROM LANDSAT TM



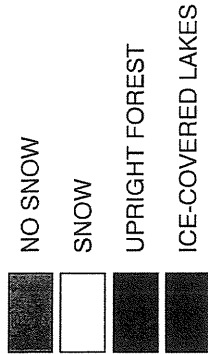
WIND DIRECTION: 255°



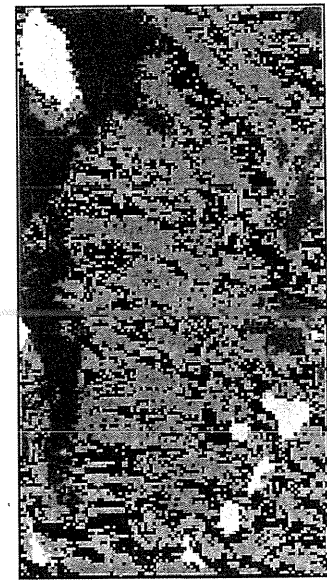
WIND DIRECTION: 240°



WIND DIRECTION: 315°



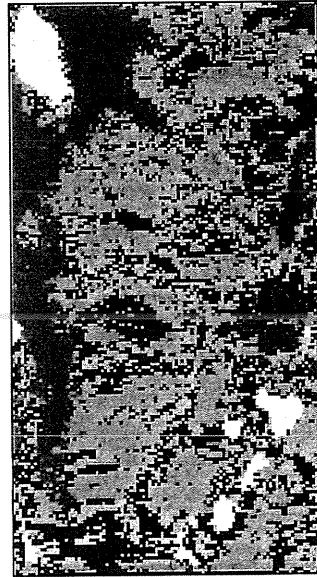
WIND DIRECTION: 225°



WIND DIRECTION: 285°



WIND DIRECTION: 270°



WIND DIRECTION: 255°



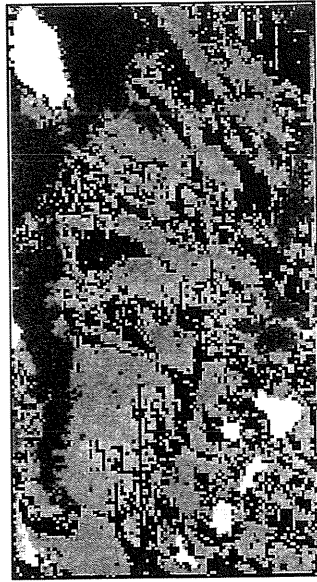
WIND DIRECTION: 300°



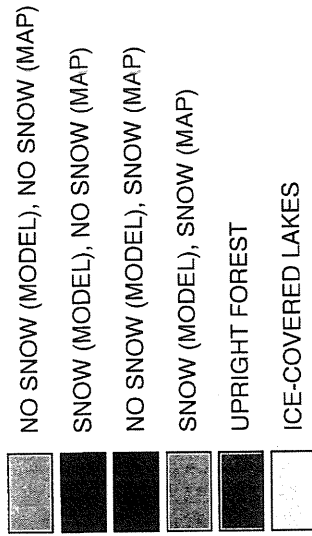
SNOWCOVER MAP, DERIVED FROM LANDSAT TM



WIND DIRECTION: 240°



WIND DIRECTION: 315°



WIND DIRECTION: 225°

### **Model-Predicted Snowcover Maps**

Maps from the seven models representing prevailing wind directions, as well as the snowcover map derived from the Landsat TM image are shown in Plate 1. No single map fully resembles the snowcover map derived from the Landsat TM image. However, several similarities between snow distribution patterns predicted by each model and the snowcover map are apparent when partial areas are considered. For example, the large snow-covered area west of Lefthand Reservoir (area "A" on the snowcover map) is predicted to varying extents by wind directions between 225° and 270°. At 285°, the representation of this area begins to break down. In the maps for wind directions of 300° and 315° only the eastern half of this area is represented. Area "B" on the snowcover map appears to resemble the predicted patterns shown on the 225°, 240°, 300°, and 315° maps, but this area is predicted to be much more fragmented in the maps for wind directions from 255° through 285°. The reader is encouraged to examine other areas of the predicted models and the snowcover map to better judge the pattern similarities. The differences among these patterns provides strong evidence for multi-directional airflow, as different areas on the snowcover map may be best represented by different wind direction models.

### **Error Maps**

Maps of errors omitted and committed by each model are shown in Plate 2. The errors associated with each model show significant spatial autocorrelation and clumping, suggesting that at least one variable is missing from the models. Recalling that the intention of this project was to examine the modeling techniques rather than develop an exhaustive alpine snow distribution model, the spatial aggregation of errors shown in Plate 2 is not surprising. As suggested above, multi-directional wind flow may be the most obvious omitted variable. However, certain areas are evident in which errors have been committed to some extent by every model, again suggesting that at least one other variable is lacking in the models. The two large dark gray areas immediately above the center of each map and the dark gray area in the lower left corner of each map provide examples of such

commission error. Omission errors common to each model appear to be less significant.

### **CONCLUSIONS**

Logistic regression models predicting the spatial extents of snowcover have been developed for each of seven characteristic prevailing wind directions for an alpine site in the Colorado Front Range. These models, designed to assess the modeling technique rather than provide definitive explanations for alpine snow distribution, suggest that the methodology is appropriate, and that further refinement is warranted. Two simple mechanistic explanatory variables were used to predict snowcover: gross topography and local topographic discontinuities. Although classification accuracies were relatively low, distinct patterns predicted by each model could be visually associated with a map of snowcover derived from a Landsat TM image. Errors resulting from these models indicated that variables were probably missing from the models, as expected. Omission errors tended to change position with wind direction, suggesting that inclusion of multi-directional airflow characteristics in the models would reduce this type of error. Several commission errors were common to all wind directions, suggesting that other variables explaining snow distribution remain to be identified.

The results of this study provide an incentive to continue the development of spatial modeling techniques to improve understanding of alpine snowcover distribution. Improvement in both quality and spatial resolution of digital elevation models is likely to be required to fully assess the spatial heterogeneity typically found in alpine snowpacks. Further development of the techniques described will need to include a method for modeling wind gradients and multi-directional airflow. Finally, the extension of these methods to predicting relative snow depth remains to be investigated. Future development of this work will require more rigorous field verification of the modeling predictions than was necessary for the exploratory nature of this project. The transient nature of snow blown by wind should certainly make that a challenging task.

## REFERENCES

- Berg, N., and N. Caine. 1975. Prediction of natural snowdrift accumulation in alpine areas. *Final Report to Rocky Mountain Forest and Range Experiment Station* (USFS 16-388-CA), Boulder, Department of Geography, University of Colorado.
- Berry, J. 1987. Fundamental operations in computer-assisted map analysis. *International Journal of Geographical Information Systems* (1), pp. 119-138.
- Holtmeir, F.K. Date Unknown. Die bodennahen winde der Indian Peaks Region, Colorado Front Range, U.S.A. Münstersche Geographische Arbeiten, Institut für Geographie, Universität Münster.
- Kobayashi, D. 1972. Studies of snow transport in low-level drifting snow. *Contributions from the Institute of Low Temperature Science, Hokkaido University, Sapporo, Japan, Series A, No. 29.* 64 pp.
- Losleben, M.V. 1983. Climatological data from Niwot Ridge, East Slope, Front Range, Colorado. *Long-Term Ecological Research Data Report 83/10; J.C. Halfpenny, Editor.* Institute of Arctic and Alpine Research, University of Colorado, Boulder.
- Odlund, J. 1988. Spatial Autocorrelation. Newbury Park: Sage Publications. 85 pp.
- Olyphant, G.A., and S.A. Isard. 1987. Some characteristics of turbulent transfer over alpine surfaces during the snowmelt-growing season: Niwot Ridge, Front Range, Colorado, USA. *Arctic and Alpine Research* (19)3, pp. 261-269.
- Pereira, J.M.C., and R.M. Itami. 1991. GIS-based habitat modeling using logistic multiple regression: a study of the Mt. Graham Red Squirrel. *Photogrammetric Engineering and Remote Sensing* (57)11, pp. 1475-1486.
- Radok, U. 1968. Deposition and erosion of snow by the wind. *Cold Regions Research and Engineering Laboratory Research Report 230.* Hanover, New Hampshire: U.S. Army.
- Schmidt, R.A. 1982. Properties of blowing snow. *Reviews of Geophysics and Space Physics* (20)1, pp. 39-44.
- Schmidt, R.A. 1986. Transport rate of drifting snow and the mean wind speed profile. *Boundary-Layer Meteorology* 34, pp. 213-241.
- Skidmore, A.K. 1989. A comparison of techniques for calculating gradient and aspect from a gridded digital elevation model. *International Journal of Geographic Information Systems* (3)4, pp. 323-334.
- Swanson, F.J., et al. 1988. Landform effects on ecosystem patterns and processes. *Bioscience* (38)2, pp. 92-98.
- Tabler, R.D. 1973. Evaporation losses of windblown snow and the potential for recovery. *Proceedings, Western Snow Conference, Grand Junction, Colorado, No. 41,* pp. 75-79.
- Takeuchi, M. 1980. Vertical profile and horizontal increase of drift-snow transport. *Journal of Glaciology* (26)94, pp. 481-492.
- Thorn, C.E. 1974. An analysis of nivation processes and their significance, Niwot Ridge, Colorado Front Range. *Unpublished Ph.D Dissertation, University of Colorado.*
- Turner, M.G., Costanza, R., and F.H. Sklar. Methods to evaluate the performance of spatial simulation models. *Ecological Modelling* (48), pp. 1-18.